Geotechnical Engineering for the Preservation of Monuments and Historic Sites III – Lancellotta, Viggiani, Flora, de Silva & Mele (Eds)

A critical evaluation of proxy measures used to quantify excavation-induced damage in masonry buildings

Yiyan Liu, Burcu Gulen, Sinan Acikgoz & Harvey Burd
Department of Engineering Science, University of Oxford, Oxford, UK

Ben Gilson
Infrastructure Geotechnics Division, Arup, London, UK

Alper Ilki
Department of Civil Engineering, Istanbul Technical University, Istanbul, Turkey

Korhan Deniz Dalgic
Department of Civil Engineering, Izmir Institute of Technology, Izmir, Turkey
Faculty of Engineering, Urla, Izmir, Turkey

ABSTRACT: Building response during nearby excavation activities (e.g., tunnelling or deep excavations) is traditionally monitored by conducting displacement measurements. These displacement data are then post-processed to determine proxy measures that are correlated to damage categories. For masonry buildings, commonly-used proxy measures include building deflection ratio, horizontal relative displacement and angular distortion; simple mechanical models and empirical rules are used to define limiting values for these proxy measures to identify and control the level of cracking in buildings during construction. This procedure has a profound influence on mitigation and construction activities, and a critical evaluation of its veracity is needed. To this end, results from a recent experimental campaign on the settlement response of half-scale masonry buildings are examined in this paper. During these tests, detailed optical measurements were conducted, allowing the calculation of absolute displacements across the façade, as well as crack opening displacements at specific locations. These measurements facilitate a direct comparison between the actual observed damage and the damage category that is indicated by the proxy measures. The comparisons highlight the limitations of existing techniques. A discussion is provided on how proxy measure calculations can be improved to deliver more reliable indications of building damage.

1 INTRODUCTION

Tunnelling and deep excavation activities lead to ground movements. Such movements, if not evaluated and controlled properly, may cause damage to nearby buildings. The definition of 'damage' varies according to structural typology and building materials. In the context of masonry buildings, damage is often quantified in terms of the presence of visible cracks on façades and walls (Burland et al. 1977; Crossrail Limited 2008; High Speed Two Limited 2017; Thames Water Utilities Limited 2014). Cracking can lead to loss of weather tightness and can impact building serviceability. Furthermore, it represents a permanent loss of cohesion and can lead to structural instability (Korswagen et al. 2019). Quantifying the extent of cracking in a building requires knowledge of the location, length and width of each crack. This presents a challenge for traditional monitoring techniques and damage quantification at a high level of detail is rarely attempted in practice.

DOI 10.1201/9781003308867-79

In practical cases, the severity of building damage due to nearby underground construction is typically quantified using an approach in which horizontal and vertical displacement data are measured at selected reference points around the building. These displacement data are then processed to determine deformation measures that are employed as proxy indices for building damage. To track and manage the level of damage experienced by the building, values of the proxy indices are compared to pre-determined trigger levels set by designers, corresponding to different assumed damage categories. There is typically a specific contingency plan which defines the actions to be taken if trigger values are exceeded. The contingency plan may require changes in construction sequence and methodology, often with significant cost implications.

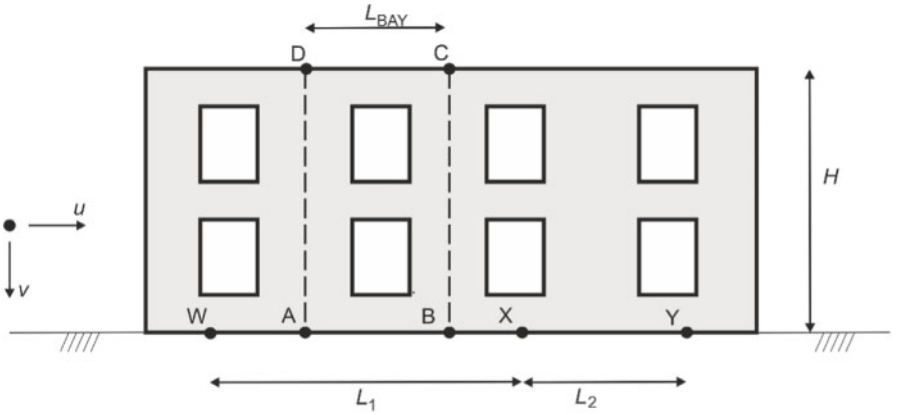

Figure 1. Example configuration of reference points to determine relative deflection, average horizontal strain and angular distortion proxy damage indices for a building façade.

'Deflection ratio' (e.g. Mair et al. 1996) is a widely used proxy index for building damage. The determination of deflection ratio values for a building façade is outlined below in terms of the example building in Figure 1. Reference points W and Y are typically selected at or close to either end of the building along the base. A query point X, where deflection ratio is assessed, is located between the reference points at the bottom of the building. Displacements u and v of the reference points and query point (where u and v signify displacement in the horizontal and vertical directions respectively) are measured during construction. The deflection ratio for point X relative to span WY is,

$$\left(\frac{\Delta}{L}\right)_{WXY} = \frac{v_X - \frac{v_W L_2 + v_Y L_1}{L_2 + L_1}}{L_2 + L_1} \tag{1}$$

where v_x, v_w and v_Y are the vertical displacements of points X, W and Y respectively.

The deflection ratio is a non-dimensional measure of the vertical displacement of point X with respect to a straight reference line between the displaced positions of W and Y. If the building deforms rigidly then the deflection ratio is zero. Three points are employed in this example but, in practical cases, a larger number of query points are typically used to determine the maximum value of deflection ratio for a particular façade.

'Angular distortion', β (e.g. Boscardin & Cording 1989) is an alternative potential proxy damage index. To determine maximum angular distortion for a particular building, the façade is idealised as a series of shear deformable rectangular 'bays', as shown in the example in Figure 1 for bay ABCD. Angular distortion represents the average shear strain in the bay as defined by the rotations of each of the four sides of the bay; these rotations are determined from the measured displacements of the bay corners. The angular distortion for bay ABCD determined in this way is,

$$\beta_{\mathrm{ABCD}} = -\frac{v_B - v_A}{L_{BAY}} + \frac{(u_D + u_C) - (u_A + u_B)}{2H} \tag{2}$$

Separately, data on the horizontal displacement of reference points located on either end of the façade or bay at the base can be used to determine values of 'average horizontal strain', ε^h. For the example case in Figure 1 the average horizontal strain, ε^h_{WY}, is determined for span WY as,

$$\varepsilon^h_{WY} = \frac{u_Y - u_W}{L_1 + L_2} \tag{3}$$

Values of deflection ratio inferred from site measurements are typically employed with a simplified elastic deep beam model of the building façade to estimate the maximum tensile strainε^t_{max} experienced by the façade (e.g. Mair et al. 1996). In cases where the measured average horizontal strains at the base of the building are tensile, then these tensile strains are also incorporated in the analysis. Values of ε^t_{max} determined in this way are related to notional building damage categories via standard correlations (see the Appendix).

Inferred values of maximum principal tensile strain ε^t_{max} are correlated with notional damage category in a similar way when angular distortion is used as a proxy measure (e.g. Son & Cording 2005). In this case the maximum tensile strain is determined straightforwardly on the basis that each bay is assumed to deform uniformly in pure shear. When the average horizontal strain at the base of the bay is tensile then the analysis is typically modified to account for the presence of this additional strain.

Proxy damage indices, and their use in damage quantification, may have a significant influence on how mitigation and construction activities are conducted. Uncertainties exist around the reliability of simplified modelling approaches employed to infer values of maximum tensile strain from proxy damage indices; such simplified models do not consider certain important aspects such as the likely influence of openings in the façade. Questions also exist, on whether values of maximum tensile strain inferred from the model can be reliably correlated with actual damage experienced by a building.

To explore the extent to which proxy damage indices provide a useful measure of actual building damage, a study on half-scale masonry buildings subjected to simulated tunnel-induced displacements has been conducted. The paper initially introduces the experimental program. Data from the experiments are then employed to explore correlations between proxy damage indices and observed building damage.

2 EXPERIMENTAL DATA

2.1 *Test building and instrumentation*

An experimental campaign on the settlement response of half-scale masonry buildings was conducted at Fibrobeton's factory site in Turkey between December 2020 and March 2021. One of the test buildings employed in the experiments, illustrated in Figure 2, is the focus of the current paper. The building comprises a pair of 2-storey masonry façades with reinforced concrete slabs placed between them at first floor and roof level. The building was constructed on two parallel steel beams connected to a manual screw jack at one end (Figure 2c). The façades were built with half-scale bricks ($115 \times 57.5 \times 30$ mm) laid in English bond. Concrete kentledge blocks weighing 8 tonnes in total were placed on the first and top floor slabs to satisfy scaling requirements. Downwards displacements were applied to the steel beams by the screw jacks to impose deformations on the building that mimicked the hogging region of a typical settlement profile caused by nearby tunnel construction.

Two separate tests were conducted on the building. In an initial test (30-RS-W1) significant gapping was observed to occur between the base of the façade and the steel beams and only minimal damage was induced in the façade. A second test (30-RS-W3) – intended to induce considerably more damage in the building - was therefore subsequently conducted on the same building with an additional 3.25 tonnes of kentledge applied to the lower windowsills. These two tests – referred to as Test 1 and Test 2 respectively in the following text - are illustrated in Figure 2a and b.

270 no. paper targets with printed concentric rings were placed on the front wall and the steel beam. The targets were monitored by four video cameras; the displacement of each target was determined using 2D Digital Image Correlation (DIC). Specifically, three cameras facing the wall were used to monitor the in-plane displacements, while the fourth camera was used to measure the out-of-plane displacements. More than 100 targets were monitored by more than one camera; this redundancy in the measurements was exploited to check the accuracy of the data. Fibre Bragg grating (FBG) cables were used to conduct additional strain measurements; these strain data were used to validate the DIC measurements.

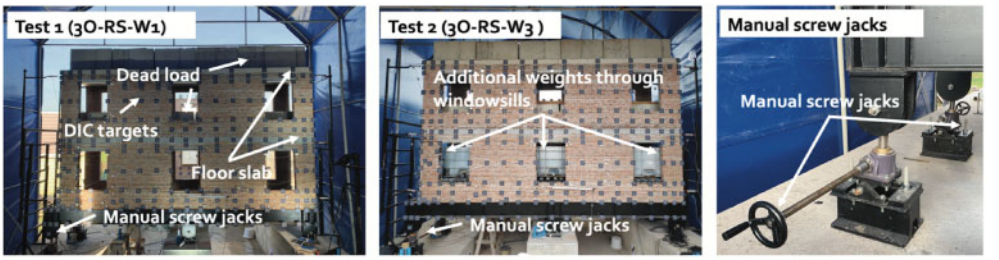

Figure 2. Test setups and weight arrangement: (a) Test 1 (3O-RS-W1); (b) Test 2 (3O-RS-W3); (c) manual screw jack arrangement; The specimen is 5.6m in length, 3.2m in height and the wall thickness is 0.115m.

Adjacent target pairs were used to form 'virtual Linear Variable Differential Transformers (LVDT)' as illustrated in Figure 3. The measured displacements of the targets were used to determine the increase in distance Δs between the targets as,

$$\Delta s = \frac{\Delta x\,(u_2 - u_1) + \Delta y\,(v_2 - v_1)}{\sqrt{\Delta x^2 + \Delta y^2}} \tag{4}$$

Positive values of Δs were taken to indicate a single crack of width Δs between the location of the two targets.

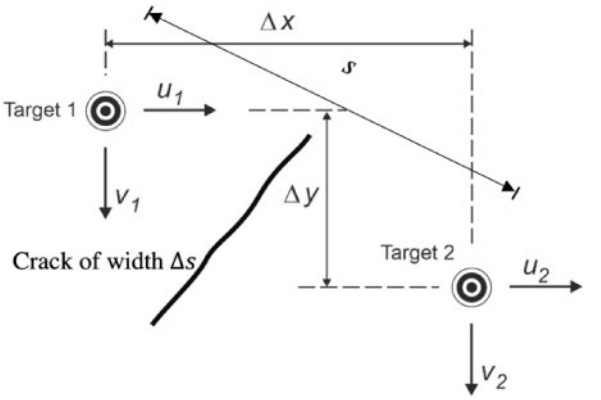

Figure 3. Arrangement employed for the 'virtual LVDTS'. Two targets are separated by distance s. The measured displacements of Target 1 and Target 2 are (u_1, v_1) and (u_2, v_2) respectively.

2.2 *Test procedures*

Tests were conducted by two operators gradually loading the steel beam via the manual screw jacks (Figure 2c) to a desired tip displacement. Once the maximum jack displacement had been applied in each test a visual inspection of the front façade was conducted to log the presence of visible cracks (a crack is considered to be visible when its width exceeds 1mm). To quantify the crack widths, sets of target pairs that spanned the visible cracks were identified. Displacement data from these target pairs were processed using the approach in Equation (4) to determine representative crack widths. The largest crack width determined in this way was considered to provide an objective measure of the actual damage experienced by the building.

In Test 1 (Figure 2a), the beam tip displacement was increased to $V_{tip} = 66.67$ mm via the screw jacks. Loading applied by the screw jacks was slowly removed once the test had concluded. The test took 5 hours and 36 minutes to complete, requiring 6700 seconds of DIC recording time. The building was observed to deform approximately rigidly during the test, with gaps forming between the building and the steel beam at the building corners (as illustrated in Figure 4a). The only visual damage on the front wall was a vertical crack located on the bottom spandrel beneath window 2.

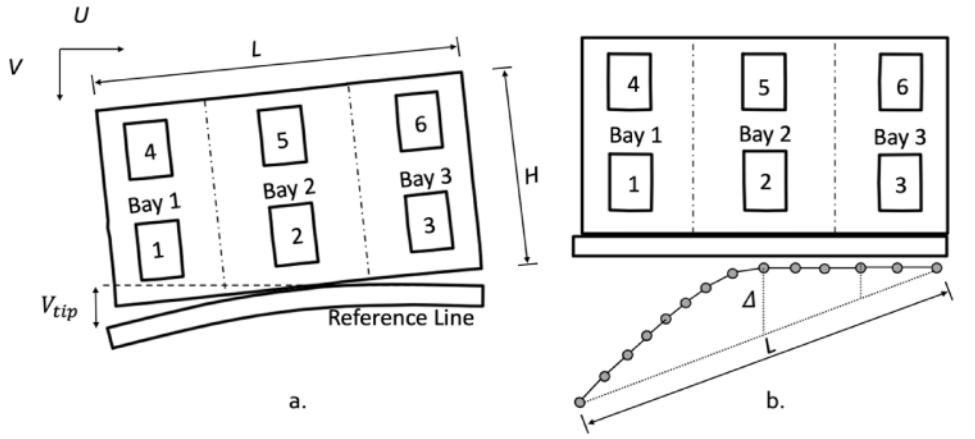

Figure 4. (a) Diagrammatic illustration of the test building showing the three bays employed for the determination of angular distortion and the vertical displacement V_{tip} applied to the steel beam supporting the building; (b) illustration of the procedure to determine the deflection ratio of (Δ/L)

In Test 2, the supporting beam was loaded to a displacement $V_{tip} = 34.9$ mm. At this value of displacement a significant amount of damage was visible and so the test was terminated. The test took 4 hours and 50 minutes to complete; the total DIC recording time was 3096 seconds.

3 EVALUATING PROXY DAMAGE MEASURES FROM THE TEST DATA

3.1 *Displacement ratio, angular distortion and average horizontal strain*

The in-plane displacement of targets placed along the base of the façade were determined by the DIC system at each time instance. This procedure provided a means of determining the profile of vertical deformations along the base of the wall as illustrated in Figure 4b. The deflection ratio with respect to the bottom two corners of the building was determined by finding the target location that maximised the value of Δ/L, employing Equation (1) as illustrated in Figure 4b. Values of average horizontal strain were determined on the basis of horizontal displacements of targets placed at the bottom corners of the building or bays.

To determine angular distortion, the building was divided into three bays as illustrated in Figure 4. Displacement data were determined from targets located at the four corners of each bay; these data were used in Equation (2) to determine the angular distortion for each bay.

3.2 *Determination of maximum tensile strain from relative deflection*

The maximum tensile strain ε^t_{max} was determined from the measured values of deflection ratio as described below (Mair et al. 1996). This procedure idealises the building as an elastic deep beam neglecting the presence of openings and floors as indicated in Figure 5.

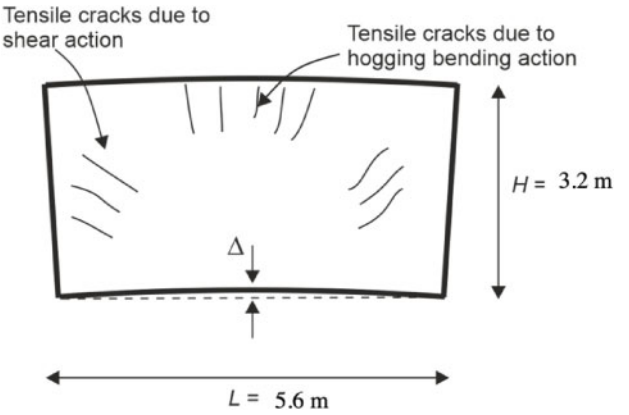

Figure 5. Assumed deformation mode and potential crack locations for elastic deep beam approximation of the building façade.

In the current tests the building is considered to deform in hogging as shown in Figure 5. Values of maximum tensile strain were determined using an elastic deep beam approximation in which the neutral axis is assumed to coincide with the base of the façade. On the basis of this approach the maximum tensile strain due to bending, ε^t_b is determined as,

$$\frac{\Delta}{L} = \left\{ \frac{L}{12H} + \frac{EH}{2LG} \right\} \varepsilon^t_b \tag{5}$$

where G and E are shear modulus and Young's modulus respectively. A separate estimate of the maximum tensile strain due to shear, ε^t_s, is given by,

$$\frac{\Delta}{L} = \left\{ 1 + \frac{GL^2}{6H^2E} \right\} \varepsilon^t_s \tag{6}$$

In the current tests the behaviour was invariably found to be bending-dominated; i.e. the largest values of horizontal strain were always those determined by Equation (5). Following Mair et al. (1996) the ratio E/G was taken to be 2.6.

Tensile strains were found to occur at the base of the building. A representative value of average horizontal strain ε^h was therefore combined additively with the value of ε^t_b determined from Equation (5) – following the procedure in Mair et al. 1996 – to obtain an estimate of ε^t_{max} (the maximum principal tensile strain experienced by the building).

Since the behaviour of the façade is predicted to be bending-dominated, tensile cracking near the top of the beam at midspan would be expected as illustrated in Figure 5. In the alternative shear-dominated case then inclined cracks would be expected at mid-height on the left and right edges of the façade, as also shown in Figure 6

3.3 *Determination of maximum tensile strain from angular distortion*

A building bay subject to a positive angular distortion (defined using the conventions in Equation 2) will deform as illustrated in Figure 6. Figure 6 also shows the expected cracks for this case.

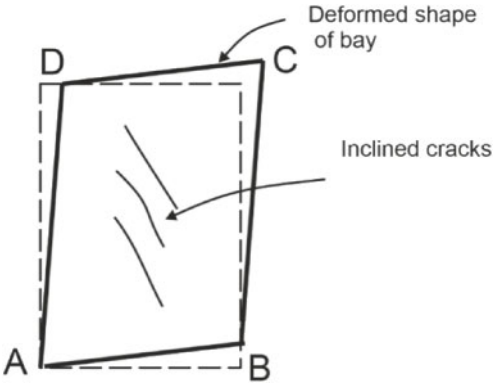

Figure 6. Expected crack pattern in a building bay with an imposed angular distortion. The inclination of the cracks will depend on the ratio between angular distortion, β, and average horizontal strain ε^h_{AB}at the base of the bay.

The maximum tensile strain associated with the angular distortion is therefore determined straightforwardly (Son & Cording 2005) as,

$$\varepsilon^t_{max} = \frac{\varepsilon^h_{AB}}{2} + \sqrt{\left(\frac{\beta}{2}\right)^2 + \left(\frac{\varepsilon^h_{AB}}{2}\right)^2} \tag{7}$$

where ε^h_{AB} is a representative value of average tensile strain for edge AB.

4 DAMAGE CLASSIFICATION ON THE BASIS OF CRACK WIDTH MEASUREMENTS

Crack patterns determined by visual inspection for both tests are shown in Figure 7; data from the 'virtual LVDTs' used to quantify the crack widths are indicated in the figure via the colour scale bar. Values of maximum crack width (determined from the 'virtual LVDTs') are listed in Table 1. 'Prototype' crack width data in Table 1 indicate the equivalent maximum crack width at prototype scale on the basis of a linear scale factor of 2. The damage classifications listed in Table 1 were determined by employing the conventional correlations between maximum crack width and damage category (see Appendix).

Table 1. Observed damage in Test 1 and Test 2.

Test code	Number of visible of cracks	Maximum crack width inferred from 'virtual LVDTs'	Prototype crack width	Damage category
Test 1	1	1.68 mm	3.36 mm	slight
Test 2	6	8.06 mm	16.12 mm	severe

In Test 1 a single crack, which ran along mortar joints, was observed in the spandrel beneath opening 2 (Figure 7a). This spandrel is subjected to a significant hogging action and the location of the crack – on the upper edge of the spandrel – is consistent with beam theory assumptions

on the location of tensile strains. For Test 2 the pattern of cracking is more complex (Figure 7b), which includes cracks along mortar joints and through bricks. In this case the damage is dominated by horizontal splits along bed joints at the top of the piers adjacent to openings 1 and 3. This splitting mechanism appears to have been driven by the additional kentledge applied to the lower windowsills in this test. The observed cracking patterns do not resemble the idealised patterns in Figures 5 and 6 that would be implied by simple models. The damage is confined to the lower level of the façade (i.e. below the first floor slab); the first floor slab appears to have acted to shield the upper level of the masonry façade from damage.

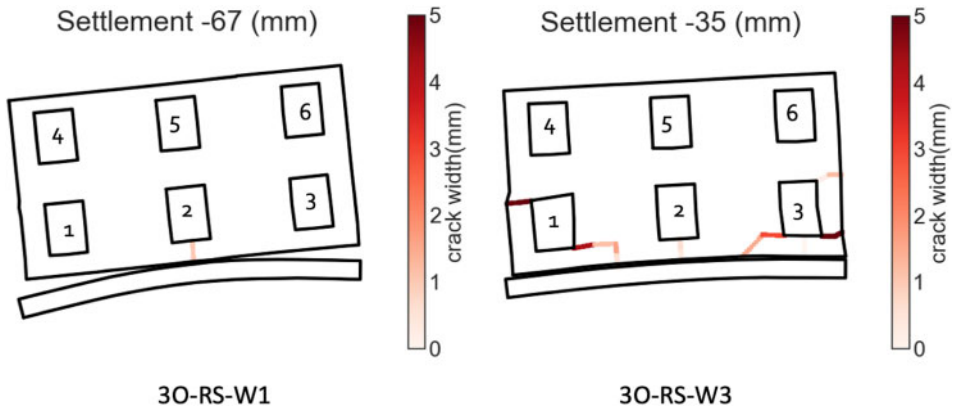

Figure 7. Illustration of the visible cracks at the end of each test (a) Test 1 (3O-RS-W1); (b) Test 2 (3O-RS-W3).

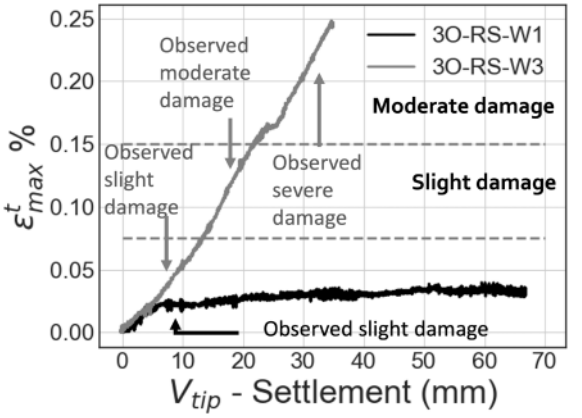

Figure 8. Values of maximum tensile strain ε^t_{max} inferred from measured values of relative deflection and average horizontal strain. Horizontal dashed lines indicate boundaries between implied damage categories (based on standard correlations, see Appendix). Vertical arrows indicate damage classification on the basis of measurements on maximum prototype crack width.

Data in Figure 8 indicate the development of maximum tensile strain ε^t_{max}, determined on the basis of measured deflection ratio and average horizontal strain. In test 3O-RS-W1 the values of ε^t_{max} appear to reach a plateau after a beam tip displacement of about 7 mm; a gap appears to have formed at the building/beam interface at this point in the test. At later stages in the test the state of deformation in the building appears to have remained broadly constant, with increases in the tip displacement merely causing the gap at the base of the building to increase.

According to the standard tensile strain – damage category correlation (see Appendix) the building would be classified as having negligible damage. However the prototype crack width of 3.36 mm actually observed in the test would signify 'slight damage'. There is therefore a noteworthy mismatch between inferred damage based on measured relative deflection and actual damage quantified in terms of maximum crack width.

Test 3O-RS-W3 experienced considerably more distortion than 3O-RS-W1. Values of ε^t_{max} plotted in Figure 8 reached a value of about 0.25% at the end of the test. The data in Figure 8 indicate a reasonably close numerical correlation between the damage category inferred from the proxy index and the damage category determined from visual measurements on the cracks. However, the modelling procedure employed in the analysis implies that cracking occurs at the top edge of the building (see Figure 5) whereas the observed cracks appear in quite different locations (see Figure 7).

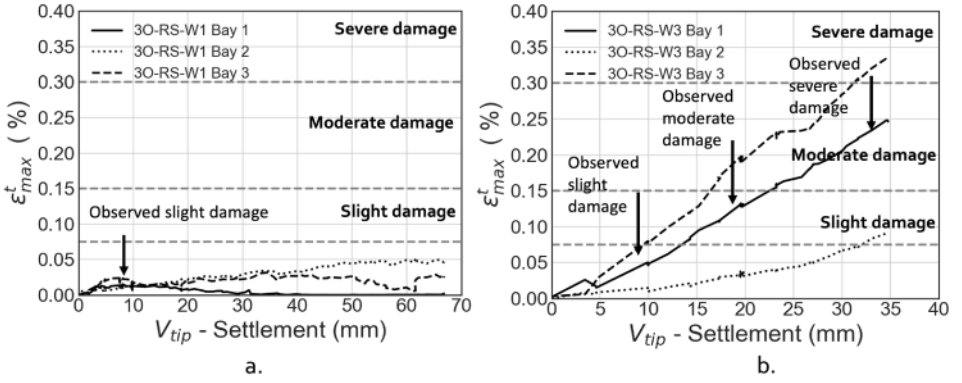

Figure 9. (a) Test 1 (3O-RS-W1); (b) Test 2 (3O-RS-W3); Values of maximum tensile strain ε^t_{max} determined from angular distortion and average horizontal strain. Black lines indicate data computed from the measured proxy indices. Horizontal dashed lines indicate boundaries between implied damage categories (based on standard correlations, see Appendix). Vertical arrows indicate damage classification on the basis of observations on maximum prototype crack width.

In Figures 9a and 9b, values of ε^t_{max} for each of the bays of 3O-RS-W1 and 3O-RS-W3 determined from the observed angular distortion (i.e. employing Equation 7) are plotted against the applied beam tip displacement. Consistent with the data in Figure 8 the angular distortion proxy measure applied to 3O-RS-W1 indicates negligible damage for all three bays. This is in contrast to the 'slight' damage category determined from crack size measurements.

Data on ε^t_{max} for 3O-RS-W3 in Figure 9b indicate significant differences between the three bays. Bay 3 experienced the greatest angular distortion. The data in Figure 9b demonstrates a fairly close numerical correlation between damage category implied by the proxy index and damage category quantified in terms of observed crack width. However, the observed cracking pattern is considerably different from the pattern predicted by the idealised model in Figure 6.

5 DISCUSSION

The adoption of simplified elastic models to represent the structural behaviour of buildings subjected to construction-induced ground movements provides a convenient and well-understood approach for the interpretation of site monitoring data on building displacements. In this approach the distortion of the building is quantified in terms of a proxy damage index (such as 'relative deflection' or 'angular distortion'). A simplified modelling approach is then used to infer a value of maximum tensile strain ε^t_{max} experienced by the building. Values of ε^t_{max} are then correlated with a notional damage category.

In numerical terms, damage categories determined on the basis of measured relative deflection combined with average horizontal strain provide a plausible correlation with objective damage measures based on direct crack width measurements. However, the observed crack patterns are entirely uncorrelated with those that would be implied by the simplified beam model employed in the interpretation process. It therefore appears that the structural behaviour of the test building is poorly represented by the simplified beam model. This finding is, of course, not unexpected. In the test building, the presence of windows, stiff floor slabs, material anisotropy and nonlinearity will – to varying degrees – cause the actual structural behaviour to depart from the assumptions implicit in the elastic deep beam modelling approach.

A similar situation was observed with the quantification of damage using measured values of angular distortion. Although numerical values of damage category determined from angular distortion data were seen to correlate fairly well with objective measures based on crack width, the overall pattern of cracking was seen to depart considerably from the assumption – implicit in the angular distortion concept - that each bay deforms in a state of pure shear.

These results – taken together – indicate the possibility that damage proxy indices of the form considered in this paper can provide useful indications of building damage. However, the data presented in the paper provide little confidence in the ability of simplified elastic models to predict realistic distributions of tensile strain. The reasonable numerical correlation between proxy damage index and observed damage is therefore likely a consequence of the relatively well-conditioned nature of the proxy measures rather than the veracity of the simplified models employed in the analysis process.

6 SUMMARY

This paper presented a case study on the performance of proxy measures (deflection ratio, angular distortion and relative horizontal displacement) on quantifying damage in a half-scale building specimen subjected to induced settlements. It was observed that the damage categories estimated by the proxy measures tend to underestimate the cracking experienced in the building. This discrepancy is not surprising and can be explained by the simplification of building behaviour with approximate deformation profiles and basic mechanical models. On the other hand, damage classification results obtained via proxy measures can clearly differentiate between damaged and undamaged specimens and estimate strains of the right order of magnitude. These are useful characteristics, particularly for quick screening of damage.

It was observed that the deflection ratio smears the localised deformation mechanisms across the whole building. However, the damage patterns observed in the buildings are typically localised and beam kinematics are not sufficient to describe building deformation mechanisms. As a result, deep beam models may lead to misleading results. Evaluation of angular distortion across building bays does not consider bending deformation and presents the opportunity to consider localised distortions. However, the choice of building bays is somewhat arbitrary, and the observed damage patterns indicate that building bays do not deform in pure shear.

From the data presented in the paper, it is clear that better discretisation of the building with more suitable mechanical models is needed to estimate strain propagation and damage from monitoring data. Local methods, which measure distortion parameters using smaller structural components, rather than measuring the whole building distortions, appear to hold more promise. Methods to estimate damage using displacement measurements from individual building components will be investigated by the authors in future research.

ACKNOWLEDGEMENT

This research was funded by the Engineering and Physical Sciences Research Council (EPSRC) of the United Kingdom and Arup Group Ltd through the iCASE project (Project Reference: 2280800).

The large-scale settlement test was performed on the Fibrobeton site in Duzce, Turkey, and the authors want to thank Fibrobeton for their support.

REFERENCES

Burland, J.B., Broms, B.B., De Mello, V.F.B., 1977. Behavior of foundations and structures. In: Proc., 9th Int. Conf. on Soil Mechanics and Foundation Engineering. Tokyo, pp. 495–546.

Crossrail Limited, 2008. Crossrail Information Paper D12 – Ground Settlement [WWW Document]. URL http://74f85f59f39b887b696f-ab656259048fb93837ecc0ecbcf0c557.r23.cf3.rackcdn.com/assets/library/document/d/original/d12groundsettlement.pdf (accessed 7.28.20).

High Speed Two Limited, 2017. High Speed Two Phase One C3?: Ground Settlement [WWW Document]. URL https://assets.publishing.service.gov.uk/government/uploads/system/uploads/attachment_data/file/672194/C3_-_Ground_Settlement__v1.pdf (accessed 7.28.20).

Korswagen, P.A., Longo, M., Meulman, E., Rots, J.G., 2019. Crack initiation and propagation in unreinforced masonry specimens subjected to repeated in-plane loading during light damage. Bull. Earthq. Eng. 17, 4651–4687.

Mair, R.J., Taylor, R.N., Burland, J.B., 1996. Prediction of ground movements and assessment of risk of building damage due to bored tunnelling. Geotech. Asp. Undergr. Constr. Soft Gr. 713–718.

Son, M., Cording, E.J., 2005. Estimation of Building Damage Due to Excavation-Induced Ground Movements. J. Geotech. Geoenvironmental Eng. 131, 162–177.

Thames Water Utilities Limited, 2014. Thames Tideway Tunnel Settlement Information Paper [WWW Document]. URL https://www.tideway.london/media/3075/app191-settlement-information-paper-3-march-2014.pdf (accessed 7.28.20).

APPENDIX

Table 2. Classification tables for masonry building damage (based on the work of Mair et al. 1996).

Damage category	Normal degree of severity	Description of typical damage	Approximate crack width (mm)	Range of maximum tensile strains (ε^{t}_{max})
0	Negligible	Hairline cracks	<0.1	0–0.05
1	Very slight	Fine cracks easily treated during normal redecoration. Perhaps	0.1–1	0.05–0.075
2	Slight	Cracks easily filled.	1–5	0.075–0.15
3	Moderate	Cracks may require cutting out and patching.	5–15 or severe >3	0.15–0.3
4	Severe	Extensive repair involving removal and replacement of sections of walls.	15–25 also depends on numbers of cracks	>0.3
5	Very severe	Major repair required involving partial or complete re-construction.	>25 depends on numbers of cracks	–